Molecular Dynamics and Free Energy Calculations on the Peculiar Bimodal Alkali Ion Selectivity of an 8-Subunit Cavitand

Christopher I. Bayly* and Peter A. Kollman

Contribution from the Department of Pharmaceutical Chemistry, School of Pharmacy, University of California, San Francisco, California 94143

*Received August 21, 1992**

Abstract: Molecular dynamics (MD) and free energy calculations were used to examine the cation selectivity of the cavitand **1**. This cavitand and two close analogs are the only macrocyclic ionophores known to date that exhibit dual ion selectivity. Experimentally,[1] the strongest binding affinity among the alkali cation series Li^+–Cs^+ is shown toward Cs^+, which is of approximately complementary size to the cavity. However, there is also a second, weaker preference for binding Na^+ over Li^+ or K^+. Free energy calculations were carried out on a fully solvated host–guest system for all the alkali cations, starting from a conformation identical to the highly symmetrical structure found for the **1**–Cs^+ complex. The calculated binding affinities reproduced the bimodal alkali ion selectivity exhibited by **1**, giving semiquantitative agreement with the experimental results. Analysis of these studies and further MD studies suggest that for Li^+–Rb^+, two water molecules accompany the ion in the cavity of the host molecule. However, only in the case of Na^+ is there an optimal arrangement of both the ion and the two waters in the cavity, thus stabilizing it compared to K^+ and Li^+.

Introduction

The development of host–guest chemistry has opened up many exciting opportunities for translating structural control over a synthetic macrocycle into powerful chemical control in terms of stereoselectivity and reactivity.[2] Compared to the biological systems they often mimic, the structure of the active site of these synthetic macrocycles is simpler and easier to predict using conventional modeling techniques (e.g. hand-held CPK models, molecular mechanics). This in turn permits a much higher degree of predictiveness in designing a host macrocycle *de novo* with a specific activity in mind.

Because of the greater conformational freedom of macrocycles compared to smaller synthetic molecules, conformational control plays an important role in this chemistry. Ideally, in trying to design a host macrocycle to adopt a certain "active" conformation in complexing with the guest, it would be desirable to know at the planning stage of the synthesis what conformational effects a certain structural change would introduce. Of course, with experimental structure determination methods the host must be synthesized beforehand, giving this information only a *posteriori*.

One response to this conundrum has been the concept of preorganization in the synthesis of the host molecule: to introduce structure into the host at the level of the organic synthesis that systematically and predictably removes the extra flexibility normally present in a macrocyclic molecule, leaving it in the "active" conformation as rigidly as possible.[2] This approach has met with a great deal of success in the area of ion complexation,[2] in general showing that the more "preorganized" rigidity there is present in the macrocycle, the more pronounced and (qualitatively) predictable its ion selectivity.

Alternatively, theoretical studies of host–guest systems in principle offer the possibility of obtaining structural information about a candidate host–guest system prior to the synthetic effort of constructing the host. The difficulty here is in obtaining dependable results having predictive value. To this end, the modeling of known systems is a means of evaluating and validating new and developing modeling methods, as well as interpreting the known data and gaining further insight into the behavior of these systems.

Toward this latter purpose have been directed a number of previous studies looking at the dynamic behavior of various crown ethers and related macrocycles and their selectivity toward the alkali cations.[3] Experimentally, the hosts examined in these studies exhibited the commonly encountered size-based selectivities, where the active site is of optimal size for one of the alkali cations, and cations progressively bigger or smaller bound progressively worse. These studies were able to reproduce at least qualitatively the observed trends in selectivity, as well as address structural issues such as the shape of the active site in the condensed phase (of particular interest in the case of the very flexible 18-crown-6 host, and its derivatives) and its solvation.

A deeper challenge is presented by the complexation behavior of cavitand **1**. This 8-unit ionophore is symmetrically and rigidly preorganized[1] to have a binding cavity complementary to a large ion such as Cs^+, which is the experimentally most preferred guest among the alkali ions. However, ther is also an additional (i.e. secondary) preference shown for Na^+ over both the next smallest (Li^+) and next largest (K^+) alkali ion, by 1.8 and 1.2 kcal/mol, respectively. This peculiar behavior, shared only by two other

* Permanent address: Merck Frosst Canada Inc., C.P. 1005 Pointe Claire—Dorval, Quebec, H9R 4P8, Canada.

• Abstract published in *Advance ACS Abstracts*, December 15, 1993.

(1) Cram, D. J.; Carmack, R. A.; deGrandpre, M. P.; Lein, G. M.; Goldberg, I.; Knobler, C. B.; Maverick, E. F.; Trueblood, K. N. *J. Am. Chem. Soc.* **1987**, *109*, 7068.

(2) (a) Cram, D. J. *Science* **1988**, *240*, 760. (b) Lehn, J.-M. *Angew. Chem., Int. Ed. Engl.* **1988**, *27*, 89.

(3) (a) Miyamoto, S.; Kollman, P. A. *J. Am. Chem. Soc.* **1992**, *114*, 3668. (b) Maye, P. V.; Venanzi, C. A., *J. Comp. Chem.* **1991**, *12*, 994. (c) Boudon, S.; Wipff, G. *J. Chim. Phys. Phys.-Chim. Biol.* **1991**, *88*, 2443. (d) Auffinger, P.; Wipff, G. *J. Chim. Phys. Phys.-Chim. Biol.* **1991**, *88*, 2525. (e) Dang, L. X.; Kollman, P. A. *J. Am. Chem. Soc.* **1990**, *112*, 5716. (f) Mazor, H. M.; McCammon, J. A.; Lybrand, T. P. *J. Am. Chem. Soc.* **1990**, *112*, 4411. (g) Grootenhuis, P. D.; Kollman, P. A. *J. Am. Chem. Soc.* **1989**, *111*, 55. (h) Gehin, D.; Kollman, P. A.; Wipff, G. *J. Am. Chem. Soc.* **1989**, *111*, 3011. (i) Grootenhuis, P. D.; Kollman, P. A. *J. Am. Chem. Soc.* **1989**, *111*, 2152. (j) Grootenhuis, P. D.; Kollman, P. A. *J. Am. Chem. Soc.* **1989**, *111*, 4046. (k) van Eerden, J.; Harkema, S.; Feil, D. *J. Phys. Chem.* **1988**, *92*, 5076. (l) Lybrand, T. P.; McCammon, J. A.; Wipff, G. *Proc. Natl. Acad. Sci. U.S.A.* **1986**, *83*, 833.

(4) Cram, D. J.; Kaneda, T.; Helgeson, R. C.; Brown, S. B.; Knobler, C. B.; Maverick, E. F.; Trueblood, K. N. *J. Am. Chem. Soc.* **1985**, *107*, 3645.

0002-7863/94/1516-0697$04.50/0

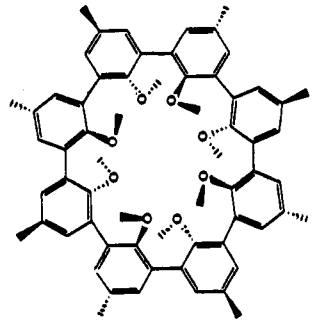

1

very closely related 8-unit macrocycles,[1,5] represents a notable exception to the otherwise well-behaved size-based selectivities that have been the hallmark of this genre of macrocyclic host. Indeed, **1** is the 8-unit analog of a series of 6-unit spherands each of which demonstrated a single, very strong, size-based selectivity toward one of the alkali ions.[4] Each of these 6-unit spherands exhibited a highly symmetric and rigidly preorganized structure similar to that of cavitand **1**, only smaller. What then is the structural basis for the secondary preference of **1** for Na^+? What are the implications with regards to the concept of selectivity based on size complementarity? To try and answer these questions, this work incorporates recently developed refinements in free energy simulation methodology in attempting to reproduce this peculiar and subtle effect.

Theory

Free energy simulations are used to calculate the change in free energy in going from a system in state A to the corresponding system in state B. This is done by gradually changing state A into state B by using a coupling parameter (λ) to smoothly convert the potential energy description (V_A) of state A ($\lambda = 0$) into the potential energy description (V_B) of state B ($\lambda = 1$), using a linear combination of V_A and V_B (eq 1) to define the potential energy (V_λ) at any value of λ.

$$V_\lambda = \lambda V_A + (1 - \lambda) V_B \tag{1}$$

The free energy of this change can then be evaluated using thermodynamic integration[6] (eq 2), integrating over the conversion coordinate λ.

$$\Delta G = G_{\lambda=1} - G_{\lambda=0} = \int_0^1 \left\langle \frac{\partial V_\lambda}{\partial \lambda} \right\rangle_\lambda d\lambda \tag{2}$$

The angle brackets denote a statistical average, with the subscript λ indicating that the average is taken from the MD ensemble generated from the Hamiltonian based on V_λ. An isothermal–isobaric (NPT) ensemble is necessary in order to obtain a Gibbs free energy. The average is taken of the derivative of the Hamiltonian with respect to λ, which for the NPT ensemble corresponds to the derivative of V_λ as indicated above. The approach used in this work was to evaluate $\partial V_\lambda/\partial\lambda$ analytically for each configuration, building up the statistical average by sampling many configurations from an MD trajectory based on V_λ. Since the statistical averages are numerical the integration cannot be performed analytically, so instead a numerical integration is carried out over points evaluated at a number of discrete intermediate values of λ (or "windows").[7] Integration over n windows using the trapezoid rule is employed here (eq 3).

$$\Delta G = \sum_{i=0} \frac{\left\langle \frac{\partial V_{\lambda_{i+1}}}{\partial \lambda} \right\rangle_{\lambda_{i+1}} + \left\langle \frac{\partial V_{\lambda_i}}{\partial \lambda} \right\rangle_{\lambda_i}}{\lambda_i - \lambda_{i+1}} \tag{3}$$

It is important to distinguish thermodynamic integration as used here from the so-called "slow growth" method, which uses a finite difference approximation to eq 2. A single MD trajectory joins the initial to the final state, with λ continuously changing at each step. The "slow growth" method does not sample the configuration space as effectively as thermodynamic integration,[8] and a "lag time" of the system toward the Hamiltonian has been shown to occur.[9]

In previous versions of AMBER,[10] only statistical perturbation ("windows") and slow growth free energy methods were implemented. We have found the thermodynamic integration method to give more accurate and reversible free energies than perturbation or slow growth for a given length trajectory in calculating the relative solvation free energy of Li^+ to Cs^+ in water.[8]

By using thermodynamic integration to obtain the Gibbs free energy change between two states, relative binding free energies can be calculated from the thermodynamic cycle shown in Figure 1. Here, the desired free energy change is depicted by the horizontal arrows, where guest 1 and guest 2 move from solution to bind to the host; the relative binding free energy is $\Delta G_2 - \Delta G_1$. In general, this event occurs on much too long a time scale to be effectively simulated with current techniques, although PMF approaches have been used.[3e] Instead, the unphysical process depicted by the vertical arrows is simulated, i.e. guest 1 is "mutated" to guest 2 in solution and in the host to obtain ΔG_3 and ΔG_4. Taking advantage of the fact that the free energy change between two states is independent of the path taken to go from one state to the other, the relative binding free energy can then be calculated as $\Delta G_4 - \Delta G_3$.

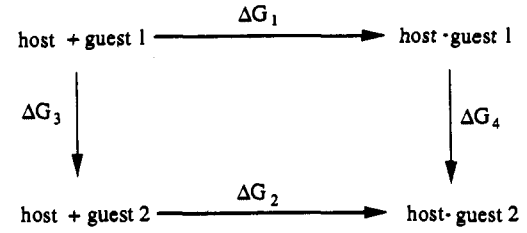

Figure 1. Thermodynamic cycle used to determine the relative free energy of binding between two host–guest complexes.

Table 1. Force Field Parameters for the Alkali Cations

cation	R^* (Å)	ϵ (kcal/mol)
Li^+	1.137	1.83×10^{-2}
Na^+	1.868	2.77×10^{-3}
K^+	2.658	3.28×10^{-4}
Rb^+	2.956	1.71×10^{-4}
Cs^+	3.395	8.06×10^{-5}

Methods

All calculations were carried out with the AMBER force field and the AMBER 4.0 molecular dynamics package.[10] The all-atom parameters and atomic charges used for the anisole unit were taken from refs 11 and

(5) Helgeson, R. C.; Mazaleyrat, J.-P.; Cram, D. J. *J. Am. Chem. Soc.* **1981**, *103*, 3929.
(6) Beveridge, D. L.; Capua, F. M. In *Computer Simulation of Biomolecular Systems*; van Gunsteren, W. F., Weiner, P. K., Eds.; ESCOM: Leiden, The Netherlands, 1989.
(7) (a) Mezei, M.; Swaminathan, S.; Beveridge, D. L. *J. Am. Chem. Soc.* **1978**, *100*, 3255. (b) Brooks, C. L., III In *Computer Simulation of Biomolecular Systems*; van Gunsteren, W. F., Weiner, P. K., Eds.: ESCOM: Leiden, The Netherlands, 1989. (c) Straatsma, T. P.; McCammon, J. A. *J. Chem. Phys.* **1991**, *95*, 1175.
(8) Bayly, C. I. Unpublished results.
(9) Pearlman, D. A.; Kollman, P. A. *J. Chem. Phys.* **1989**, *91*, 7831.
(10) (a) Pearlman, D. A.; Case, D. A.; Caldwell, J. A.; Seibel, G. L.; Singh, U. C.; Weiner, P.; Kollman, P. A. *AMBER 4.0*; University of California, San Francisco, 1991. (b) Radial distribution functions were evaluated using the CARNAL trajectory analysis module written by Wilson S. Ross for AMBER 4.
(11) Kollman, P. A.; Singh, U. C. *J. Am. Chem. Soc.* **1985**, *107*, 2212.

Table 2. Relative Free Energies of Hydration for the Alkali Cations

system	ΔΔG forward	ΔΔG backward	ΔΔG av[a]	ΔΔG Aqvist[b]	ΔΔG exp[c]
$Li^+ \rightarrow Na^+$	25.50	−25.61	25.55 ± 0.06	23.7	23.9
$Na^+ \rightarrow K^+$	17.38	−17.24	17.31 ± 0.07	17.6	17.6
$K^+ \rightarrow Rb^+$	5.48	−5.58	5.53 ± 0.05	5.4	5.1
$Rb^+ \rightarrow Cs^+$	7.80	−7.95	7.87 ± 0.08	7.8	7.7

[a] Average = $(\Delta\Delta G_{forward} - \Delta\Delta G_{backward})/2$. [b] Reference 12. [c] Reference 14.

Table 3. Comparison of Cs^{+} **1** between Minimized and Crystal[a] Structures[b]

structural feature	exp	calc
Ar–Ar dihedral angle[c]	65	73
tilt of Ar's from best plane	36	40
Ar–O–CH3 bond angle	113.0	114.7
O distances from mean plane[d]	0.99	1.11
O–O distance for opposing oxygens	6.19	6.32
Cs^+–O distance	3.24	3.35

[a] Reference 1. [b] All distances in angstroms and all angles in degrees. [c] Defined by Ar–Ar linking carbons. [d] Mean plane of all eight oxygens.

3a; the ion parameters were adapted from ref 12 (see Table 1), and the TIP3P water model[13] was used throughout. The molecular dynamics (MD) and free energy simulation studies used a time step of 2.0 fs, an 8.0-Å cutoff, a dielectric constant of 1.0, periodic boundary conditions, and an isothermal/isobaric ensemble of 300 K and 1 atm through coupling to temperature and pressure baths having coupling constants of 0.1 in each case. The solvent and solute were coupled to separate temperature baths. All the free energy simulations in this work were carried out with the spacing between windows set at $\Delta\lambda = 0.5$; 21 windows in all were used in all to go from the initial to the final state. In all cases except two (described below), in each window equilibration was carried out for 250 steps (0.5 ps) followed by data collection for 500 steps (1.0 ps); the total simulation time was thus 31.5 ps.

The aqueous alkali cation systems were constructed by immersing K^+ in a 18 Å cubic box containing 189 TIP3P waters, removing waters within 3 Å of the ion. This system was equilibrated for 10 ps, giving very stable total energy, and then mutated to the corresponding Na^+ and Rb^+ systems. The Na^+ and Rb^+ systems resulting from these simulations were each equilibrated for 10 ps before being mutated back to K^+. The equilibrated Na^+ system was mutated to the corresponding Li^+ system, which was also equilibrated for 10 ps before carrying out the reverse free energy simulations. The Rb^+ to Cs^+ free energy simulations were done similarly.

The cavitand–Cs^+ system was model built based on the highly symmetric D_{4d} crystal structure given in ref 1. This structure was then minimized to a gradient norm of less than 0.1 kcal/mol per Å. To generate the solvated host–guest systems, the minimized cavitand–Cs^+ system was placed in a rectangular flat box of TIP3P water (removing those within 3 Å of the solute), allowing 10 Å of solvent between the solute and the walls of the periodic box; this gave an initial box size of 35.8 × 35.8 × 27 $Å^3$ containing 973 solvent molecules. Equilibrating this system for 5 ps resulted in the host–guest complex tilting with respect to the box, with the possibility that future simulations would cause the solute to "see itself" along the short dimension of the box. To reduce the likelihood of this happening, the system was further equilibrated for 5 ps, with the solute biased toward a centered position using 2.0 kcal/mol per Å Cartesian constraints on the anisole-bridging carbons. After this, an additional 10 ps of unconstrained equilibration did not result in significant tilting or translation from the center of the box. The potential energy of the system was very stable, indicating adequate equilibration for our purposes. The final coordinates and velocities for the equilibrated cavitand–Cs^+ system were used as the initial coordinates and velocities for the cavitand–Rb^+ system. An initial 5 ps of equilibration was carried out with the coordinates constrained as for the cavitand–Cs^+ system above, followed by 10 ps of unconstrained equilibration, giving an energetically stabilized system. In the same fashion, the cavitand–K^+ system was generated and equilibrated starting from the final coordinates and velocities for the cavitand–Rb^+ system, the cavitand–Na^+ system from the cavitand–K^+ system, and the cavitand–Li^+ system from the cavitand–Na^+ system. These were used for the subsequent free energy calculations; thus the trajectory for a given forward simulation (e.g. starting from cavitand–Cs^+ and mutating to cavitand–Rb^+) was independent of that of the corresponding reverse simulation (starting from the cavitand–Rb^+ system and mutating to cavitand–Cs^+).

For both the forward and reverse cavitand–Na^+ to cavitand–K^+ simulations, two other sets of simulations were carried out in addition to the 31.5-ps runs mentioned above. The only changes were in the number of steps of equilibration and data collection in each window, resetting them to 250 (0.5 ps) and 750 (1.5 ps), respectively, in one case (total simulation time 42 ps), and 500 (1.0 ps) and 1000 (2.0 ps), respectively, in the other (total simulation time 63 ps). Forty-picosecond MD production runs were carried out on the systems having Na^+, K^+, and Rb^+ bound to the cavitand. For the aqueous Na^+ and K^+ systems, 20-ps production runs were carried out. Coordinate sets were taken every 0.1 ps for the production runs.

Table 4. Relative Free Energies of Alkali Ion Complexes with **1**

system	length of run (ps)	ΔΔG forward	ΔΔG backward	ΔΔG av[a]
$Li^+ \rightarrow Na^+$	31.5	22.90	−21.71	22.3 ± 0.6
$Na^+ \rightarrow K^+$	31.5	19.21	−16.96	18.1 ± 1.1
	42.0	18.28	−17.27	17.8 ± 0.5
	63.0	18.46	−18.52	18.5 ± 0.3
$K^+ \rightarrow Rb^+$	31.5	5.00	−5.25	5.1 ± 0.1
$Rb^+ \rightarrow Cs^+$	31.5	6.64	−6.32	6.5 ± 0.2

[a] Average = $(\Delta\Delta G_{forward} - \Delta\Delta G_{backward})/2$.

Table 5. Relative Free Energies of Binding for Alkali Ions to **1**

system	ΔΔG exp[a]	ΔΔG calc
$Li^+ \rightarrow Na^+$	−1.8	−3.3 ± 0.1
$Na^+ \rightarrow K^+$	+1.2	+1.2 ± 0.1
$K^+ \rightarrow Rb^+$	−1.5	−0.4 ± 0.1
$Rb^+ \rightarrow Cs^+$	−3.5	−1.4 ± 0.3

[a] Reference 1; reported values are averages of two values falling within 0.3 kcal/mol of each other.

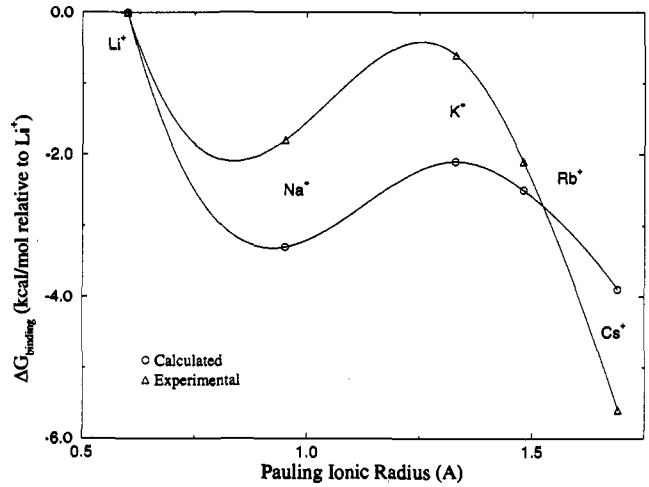

Figure 2. Plot of calculated (○) and experimental (△) $\Delta G_{binding}$ relative to Li^+ for complexes of **1** with Li^+, Na^+, K^+, Rb^+, and Cs^+. The calculated values are derived from the calculated ΔΔG values in Table 5. Note the bimodal alkali ion selectivity in both cases.

Results and Discussion

The free energy simulations on the aqueous alkali cations resulted in relative free energies of hydration, given in Table 2, that compared well with experiment[14] as well as with the previous work involved in the cation parametrization.[12] The alkali ion parameters used here were developed previously as a completely effective potential based on explicit SPC waters as solvent, using

(12) Aqvist, J. *J. Phys. Chem.* **1990**, *94*, 8021.
(13) Jorgenson, W. L.; Chandrasekhar, J.; Madura, J. D. *J. Chem. Phys.* **1983**, *79*, 926.
(14) Burgess, M. A. *Metal Ions in Solution*; Ellis Horwood: Chichester, England, 1978.

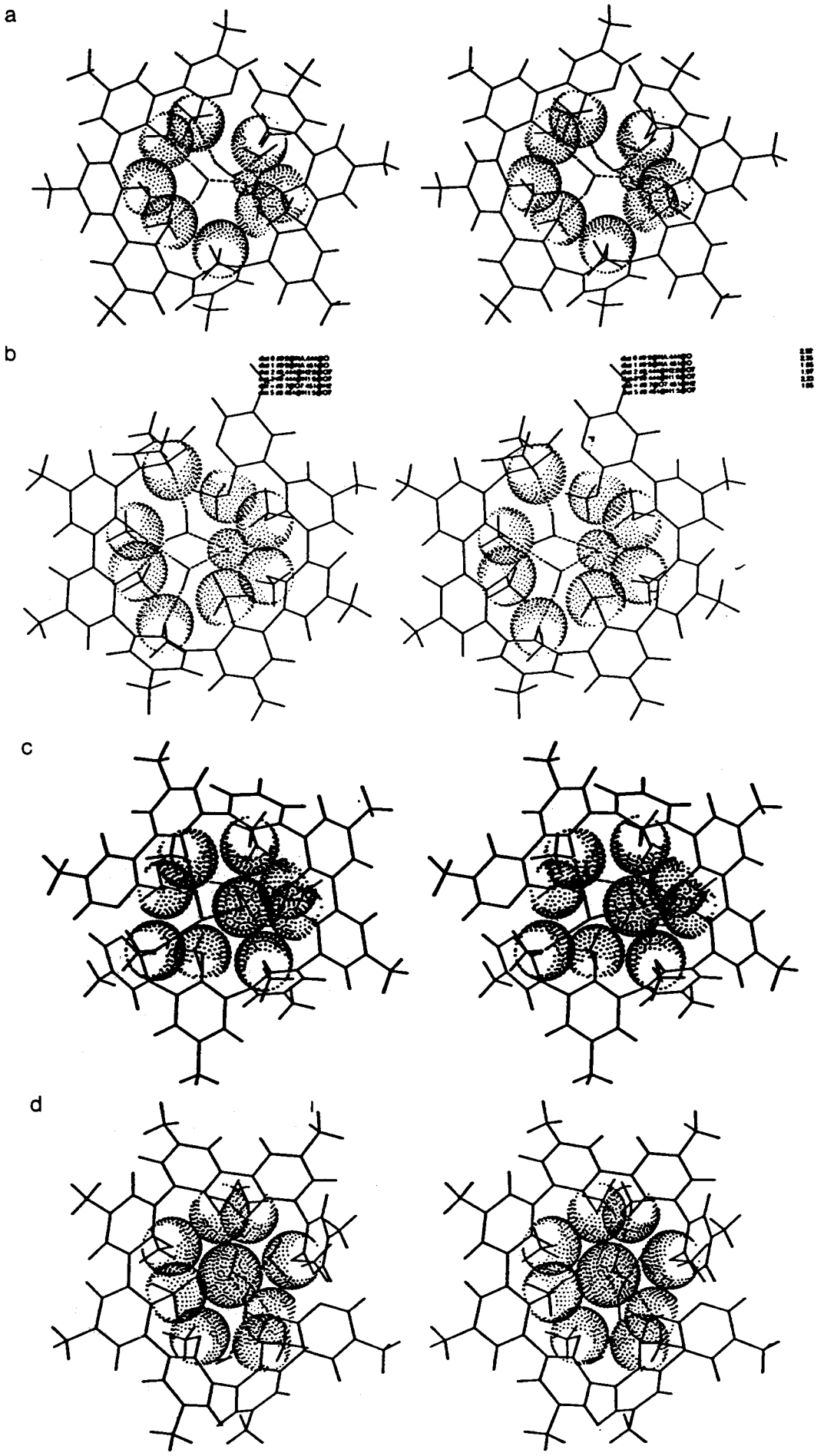
a
b
c
d

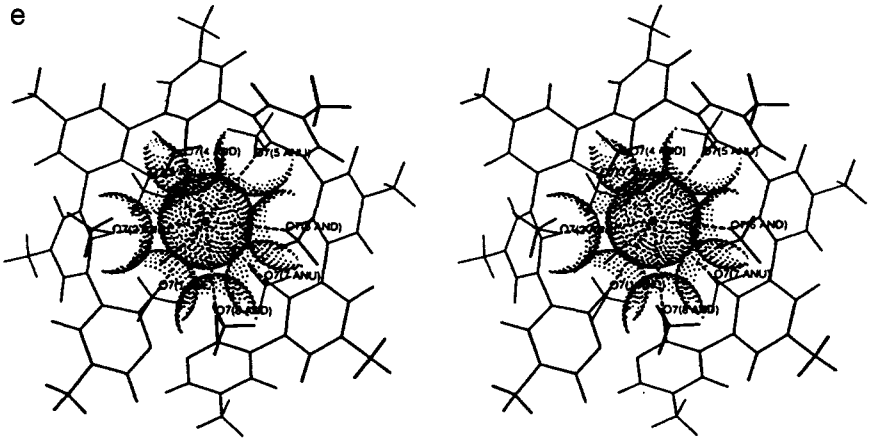

Figure 3. MD snapshots of the (a) Li^+, (b) Na^+, (c) K^+, (d) Rb^+, and (e) Cs^+ complexes with **1**. For clarity, no solvent molecules except for the two active site waters are shown. The exposed van der Waals surfaces of the ion and the cavitand oxygens are indicated, and hydrogen bonds between the active site waters are given by dashed lines, as are some of the ion–oxygen interactions.

the surface-constrained all-atom model with no nonbonded cutoff.[15] The criterion for the parametrization was to reproduce the absolute hydration free energies of the ions as well as the radial distribution functions (rdf). Although the methodology of that work differed considerably from that used here, the results confirm that these parameters also perform very well using TIP3P water, periodic boundary conditions, and an 8-Å cutoff.

Minimizing the model-built cavitand–Cs^+ complex gave a structure very similar to the crystal structure given in ref 1, by comparison of the structural features listed in Table 3. The high degree of symmetry is preserved, as is the "all out" arrangement of the methyl ether groups, and the Cs^+ ion rests in the center interacting symmetrically with all eight cavitand oxygens. The minor differences in the calculated vs experimental values in the table are mostly due to the aromatic residues having a slightly larger tilt angle in the minimized structure compared to the crystal structure.

For the solvated systems, some justification needs to be given for choosing to carry out the simulations in pure water as a solvent, instead of water-saturated chloroform which was the solvent used in getting the experimental binding data. There were two reasons for choosing pure water: First, the composition of the water-saturated chloroform used experimentally is not known. This is because in the procedure used, water saturation is carried out in the presence of the ions, which will increase the proportion of water in the actual solvent mixture compared to the known proportions for a pure water–chloroform mixture. Thus, using the latter proportionality would certainly underestimate the amount of water present. This is important because the ions would act as water scavengers in the chloroform, creating a substantially water-enriched environment around the free and cavitand-bound cations. Second, this water-scavenging process would greatly increase the equilibration times required for the simulations. Also, fluctuations at the boundary of the ion–water aggregates would further increase the statistical "noise" in the accumulated energy values while having little impact on the overall statistically averaged value. Since a mixed water–chloroform solvent was deemed impractical, pure water was used instead because the cation size changes under study would be occurring in an immediate environment which would be principally aqueous.

The final results of the free energy calculations on the solvated host–guest systems are given in Table 4, and the calculated relative free energies of binding ($\Delta\Delta G$'s) are compared with experiment in Table 5. Each value given in the tables is the average between forward and backward runs; the error represents the "hysteresis" error between the two runs. From Table 5 can be obtained the calculated $\Delta G_{binding}$ relative to Li^+ for the rest of the ions; these are plotted along with the corresponding experimental values in Figure 2. The simulations reproduced the secondary preference for Na^+ as well as the primary selectivity toward Cs^+. The low hysteresis seen in most of the runs indicates that the simulation time of 31.5 ps was adequate in general. This is not surprising in light of the conformational rigidity of the host and the strength of binding of the cation in the complex; these characteristics reduce considerably the configurational space needed for a representative sampling. It is interesting that the 31.5-ps simulation that gave the biggest hysteresis error was the Na^+ to K^+ interconversion, which is the simulation examining the secondary preference. The reasons for this became clear later on in the analysis of the results. Longer simulation times progressively reduced this error; at 63 ps of simulation the hysteresis error was only 0.03 kcal/mol between the forward and backward Na^+ to K^+ runs.

It is noteworthy that these calculations have been able to reproduce this subtle secondary binding preference for Na^+, particularly given the simplicity of the model and that the simulations were done in water rather than the experimental environment of water-saturated chloroform. A referee has pointed out that the relative binding free energies of the entire alkali series were not reproduced, i.e. calculated $\Delta G_{binding}$ relative to Li^+ (Li^+, 0.0; Na^+, = −3.3; K^+, −2.1; Rb^+, −2.5; Cs^+, −3.9) versus the corresponding experimental values (Li^+, 0.0; Na^+, −1.8; K^+, −0.6; Rb^+, −2.1; Cs^+, −5.6) (cf. Figure 2). These quantitative discrepencies obviously reflect imperfections in the model. Two likely sources of error are the use of a pure water solvent model and the omission of nonadditive (polarization) effects in the model. Since the inclusion of nonadditive effects would affect both ΔG_3 and ΔG_4 in Figure 1, it is difficult to predict what impact this would have on the above errors. The influence of nonadditive effects is being studied by Sun *et al.* (Sun, Y.; Caldwell, J.; Kollman, P. manuscript in preparation) and it is found to improve the quantitative agreement between the calculated and experimental values for the preference of a calixspherand for binding Li^+ over Na^+. Both of the above sources of error can be addressed in the future, but the fact that the simpler model used here was capable of qualitatively reproducing the bimodal alkali ion selectivity validates the use of this model to examine the chemical basis for the binding preferences.

The primary selectivity of **1** for Cs^+ is easily rationalized in conventional terms of preorganization giving rise to simple size-based selectivity. As shown in the MD snaphots of **1** with Li^+, Na^+, K^+, Rb^+, and Cs^+ in Figure 3, only the Cs^+ complex (Figure 3e) fits optimally within the host, with nearly ideal coordination with the eight anisole oxygens. Thus, Cs^+ is bound by the host in a geometry analogous to its optimal interaction with water, but without paying the significant reorganization price. This structural complementarity decreases with a decrease in ion size.

(15) King, G.; Warshel, A. *J. Chem. Phys.* **1989**, *91*, 3647.

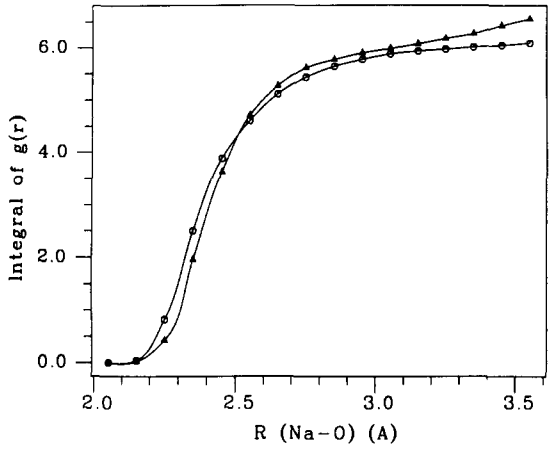

Figure 4. Integral of the radial distribution function of oxygens around Na^+ in solution (O) and in the complex (Δ).

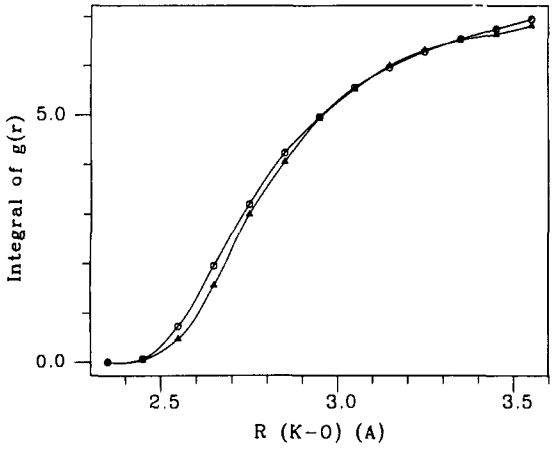

Figure 5. Integral of the radial distribution function of oxygens around K+ in solution (O) and in the complex (Δ).

This kind of primary selectivity has been understood[2] and simulated[3] many times; what is interesting and unique about this cavitand is its secondary ion selectivity for Na^+.

To try and determine the basis of the secondary preference for Na^+, the structural features of the ion binding were compared between the aqueous and host-bound systems for both Na^+ and K^+. The radial distribution function (rdf) for the ion–oxygen distances was calculated for Na^+ and K^+ both in aqueous solution and in a complex with the host. No distinction was made between solvent (water) oxygens and those of the cavitand. The integral of the rdf gives the average coordination number of oxygens to the ion as a function of distance; these are shown for the aqueous and complexed Na^+ systems in Figure 4 and for the K^+ systems in Figure 5. In each case the oxygen coordination of the aqueous and complexed systems was very similar for the first coordination sphere, (i.e. no significant structural distinction could be made between the ion binding in the host or in solution) so the secondary preference cannot be explained in terms of differential solvation of the ion between the active site and the bulk solvent.

Snapshots of the host–guest ensembles for each of the ions were examined in search of an alternative explanation, with special attention being paid to water molecules found within the cavity. With all ions, two and only two waters were found to coordinate to the complexed ion. With Cs^+ and Rb^+, these two active site waters were found more or less at the "floor" and "ceiling" of the cavity since the ions themselves were so large. With the smaller ions, the two waters gradually entered farther into the cavity. With Li^+, these two active site waters were still the only waters found inside the cavity. Interestingly, it was always the *same two waters* found in the active site in the Na^+ and K^+ systems. Since these systems were generated sequentially from the original solvated Cs^+–cavitand complex, this means that the water coordination to the cations was strong enough that exchange did not occur during the overall 50–100 ps that separated the final Na^+ and K^+ snapshots observed from the initial configuration. One of the waters did exchange part way through the MD production run on the Rb^+–cavitand complex. It is doubtful, however, that any of the active site waters would remain coordinated in solution long enough to be observed directly, e.g. by NMR.

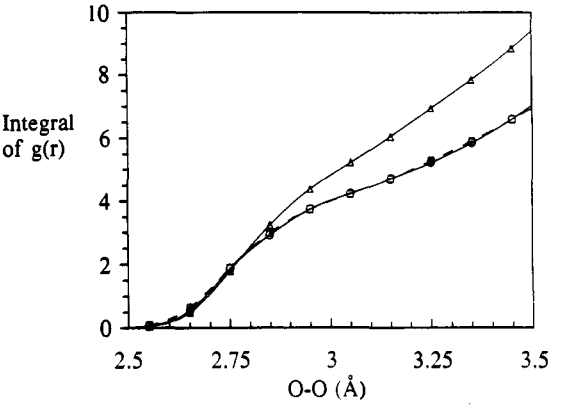

Figure 6. Integral of the radial distribution function of all oxygens (hydrogen bond acceptors) around the oxygens of the two active site waters for the Na^+ (Δ), K^+ (O), and Rb^+ (□, dashed line) complexes.

It was the hydrogen bonding of the two active site waters that provided the clearest basis for the secondary preference of the cavitand. In being drawn into the cavity by the coordination of the oxygen with the cation, the two waters are being removed from the rich hydrogen bonding environment of the bulk solution. This is compensated for by the strong oxygen–ion interaction, but further stabilization is gained by picking up as much hydrogen bonding as possible between the hydrogens of the active site waters and cavitand or solvent oxygens. In order to quantitatively assess and compare how much hydrogen bonding the active site waters were experiencing in the Na^+, K^+, and Rb^+ complexes, the rdf was evaluated for the oxygens (belonging to either host or solvent) around the active site water oxygens, since the former would be the hydrogen bond acceptors for the active site waters. For effective hydrogen bonding, the acceptor atom to donor atom distance should be about 3.1 Å or less, hence the integral of the above rdf (shown in Figure 6 for all three complexes) that falls before this distance indicates the amount of hydrogen bonding (on average) experienced by the active site waters. It is clear from Figure 6 that the Na^+ complex has approximately one extra oxygen within hydrogen bonding distance than either the K^+ or the Rb^+ complex at the 3.1-Å limit.

A structural basis for this difference presented itself upon examination of the MD trajectories and can be observed in the MD snapshots of the host–guest complexes shown in Figure 3. For both the Na^+ and K^+ complexes the ion binds to one side of the cavity, coordinating to four of the eight cavitand oxygens. The other two coordination sites of the ion are filled by the oxygens of the two active site waters. This leaves four unoccupied cavitand oxygens as hydrogen bond acceptor sites in the cavity and four hydrogen bond donors total from the two active site waters. In the case of Na^+ (Figure 3b), there is enough room left in the cavity for each water hydrogen bond donor to interact with a cavitand oxygen. However, with the larger size of K^+ (Figure 3c) there is no longer enough room in the cavity of the rigidly preorganized cavitand for both active site waters to bind to the cavitand oxygens *at the same time*. One of the two waters becomes partially disordered, retaining one hydrogen bond to a cavitand oxygen but transiently hydrogen bonding either to the other available cavitand oxygen or to solvent waters. The methoxy groups play an important role in restricting the access of the

active site waters to solvent waters. Over the course of the 40-ps MD run on the solvated K^+ complex, each of the active site waters spent some time ordered (with two hydrogen bonds to cavitand oxygens) and some time partially disordered, but at any given point in the trajectory there was one ordered and one partially disordered water. This gives rise to an explanation for the extra long simulation times needed to get a low hysteresis error in the Na^+ to K^+ free energy runs: it is likely that an important factor here was that longer times were required for the active site waters to acquire (going from K^+ to Na^+) or lose (going from Na^+ to K^+) their structural ordering. For the Rb^+ complex, the larger size of the ion simply pushed the two waters slightly farther toward the floor and ceiling of the cavity. They became somewhat more disordered due to decreased hydrogen bonding to the cavitand oxygens, and the exchange of one of the waters over the course of the simulation is also indicative of weaker binding. Nevertheless, the hydrogen bonding of the two active site waters appears from Figure 6 to be almost identical to that of the K^+ complex. The improved binding of Rb^+ compared to K^+ in the cavitand can be ascribed to better size complementarity to the cavity.

In the Li^+ complex (Figure 3a), the small size of the Li^+ allows it to form only three close interactions with anisole oxygens, completing its coordination with two waters. In contrast to the Na^+ complex, one of the waters only forms a single hydrogen bond to the anisole oxygen (the other is to an exterior water), thus two anisole oxygens do not have their hydrogen bond coordination satisfied.

Conclusions

This is the first application of free energy simulations to examine a macrocyclic host exhibiting more than a single selectivity toward the alkali cations, although a number of studies have been carried out on systems exhibiting the usual unimodal size-complementarity based selectivity.[3] Indeed, other than **1** and its two closely related analogs, we have not been able to find experimental evidence for any examples of this dual selectively among the macrocyclic alkali cation ionophores reported in the literature.[16] This work shows that the current level of force field parametrization and free energy methodologies are sufficient to reproduce both the primary and secondary preferences in the alkali cation selectivity of the cavitand **1**. The use of nonadditive potentials in the force field (especially those explicitly accounting for polarization, since these systems involve highly polar interactions) and a mixed solvent of appropriate composition could further improve the semiquantitative agreement between theoretical and experimental relative free energies of binding.

The results of this work suggest that the chemical basis for the secondary preference for Na^+ is due to the strong coordination of two active site waters to both the ion and the host in the relatively large binding cavity. In other words, the secondary preference arises from the complementarity of the cavity with the ion–water aggregate as opposed to the cavity with the ion alone. The fit of the Na^+-$2H_2O$ aggregate satisfies the available cavitand oxygen binding sites and water hydrogen bonds better than with the larger K^+-$2H_2O$ or smaller Li^+-$2H_2O$ aggregate. This is an example of a specific solvent effect, since the particular size of the solvent water molecule is a critical factor associated with its ability to fit in the active site. This suggests that a polar solvent other than water, methanol for example, could be expected to substantially alter or perhaps even remove the secondary preference for sodium. Experimental binding data for this cavitand in methanol (in either pure or mixed solvent) are not available but would be a helpful verification or refutation of this point.

It is interesting to consider the role of preorganization in the secondary selectivity for Na^+ shown by **1** as well as two other structural analogues of this cavitand which are similarly preorganized.[1,5] In the examination of the binding data for a variety of medium-sized macrocyclic ionophores containing eight electron-donating groups,[16] it was apparent that while no other examples could be found of this kind of secondary selectivity, those macrocycles were also considerably less rigid. The results of this study suggest that the designed-in rigidity of the host molecule which confers the desired primary selectivity also confers the significant energetic differentiation between ion–two water aggregates of subtly different size. If the cavitand was more flexible, it could in principle adjust to hydrogen bond to the K^+-$2H_2O$ aggregrate better. Greater flexibility of the cavity would also tend to decrease the energy gained from the better-fitting Na^+-$2H_2O$ aggregrate. If a unimodal selectivity is desired for a binding site, designing in too much "preorganized" rigidity could result in this undesirable side effect.

In summary, we feel that this study is a prototypical example of the increasing power of computer simulation methodology to give useful insight into interesting chemical phenomena. First, it was essential that the calculations at least semiquantitatively reproduced the bimodal selectivity for the alkali ions. Second, success in this first endeavor enabled the search for a structural explanation for the binding preferences, ascribed here to the preorganized structural complementarity of the cavitand **1** for Cs^+ (primary selectivity) and the Na^+-$2H_2O$ aggregate (secondary selectivity). Third, this explanation for the secondary selectivity for Na^+ clearly implicates a key and specific role of H_2O, allowing a *prediction* that this selectivity will be qualitatively altered in methanol compared to water-saturated chloroform. Thus, these studies suggest further work, both experimental and computational, that would further increase our understanding of this interesting and unusual phenomenon.

Acknowledgment. This research was supported by GM-29072 and NSF-CHE-91-13472 to P.A.K. and by a NSERC postdoctoral fellowship to C.I.B. Use of the Computer Graphics Lab (supported by RR-1081 to R. Langridge) is gratefully acknowledged.

(16) Izatt, R. M.; Pawlak, K.; Bradshaw, J. S. *Chem. Rev.* **1991**, *91*, 1721.